Communications in Physics, Vol. 33, No. 3 (2023), pp. 309-320
DOI: https://doi.org/10.15625/0868-3166/18355

Size-controlled synthesis of ZnO nanorods for highly sensitive NO_2 gas sensors

Luu Hoang Minh, **Pham Thi Thuy Thu**, **Luong Minh Tuan**, **Bui Quang Thanh**, **Mai Thi Hue**, **Ta Thi Tho and Pham Van Tong**†

Department of Physics, Faculty of Mechanical Engineering,
Hanoi University of Civil Engineering (HUCE), No. 55, Giai Phong Str., Hanoi, Vietnam

E-mail: †tongpv@huce.edu.vn

Received 20 May 2023
Accepted for publication 30 June 2023
Published 15 August 2023

Abstract. *Nanostructures of zinc oxide have been excellent potential for gas sensing applications detecting and monitoring toxic gases in the atmosphere. Appropriate nanostructures can enhance intensively the sensing performance of gas sensors. In this study, we reported the controlled fabrication of ZnO nanorods of different sizes by a simple hydrothermal method, which can be applied to detect NO_2 toxic gas efficiently. The ZnO nanorods size was controlled by adjusting amounts of D-Glucose. Morphologies and crystal structure of the synthesized materials were analyzed by the field-emission scanning electron microscopy, the X-ray diffraction patterns, and the energy-dispersive X-ray spectroscopy. The gas sensing response of the sensor based on ZnO nanorods to 2 ppm NO_2 was 13.3 and this value was 18.8 times higher than that of 500 ppm CO and NH_3, respectively. The sensor also exhibited the good selectivity and repeatability for NO_2 toxic gas with the optimum working temperature about 150˚C.*

Keywords: ZnO nanorods; hydrothermal; NO_2 gas sensors.
Classification numbers: 07.07.Df.

1. Introduction

Zinc oxide is a semiconductor metal oxide that exhibits typical n-type semiconductor properties with a wide band gap of about 3.36 eV and a large exciton binding energy ($\sim$ 61 meV) [1], which can be suitable for many other applications, such as gas sensors [2, 3], light emitting diodes [4], and solar cells [5]. ZnO based sensors are capable of detecting some toxic gases, SO_2 [6, 7], NO_2 [8, 9], NH_3 [10], CO [11], and volatile organic compounds such as ethanol,

acetone, and toluene [12]. Recently, many publications have focused on synthesizing ZnO nanostructures such as nanorods [13], nanowires [14], and nanosheets [15], studying their influence on the gas sensing performance. For instance, Fan *et al.* [16] fabricated single-crystal ZnO nanowires by chemical vapor deposition and studied the effect of wire diameter on the sensor's response to NO_2, CO, NH_3, and O_2. Jiao et al. [17] synthesized three different ZnO nanostructures by low-temperature hydrothermal growth. The results showed that the sparsely grown nanowires were effective in detecting NO_2. By a chemical vapor deposition, Liao et al. [18] successfully fabricated ZnO nanorods with different mean diameters arranged in groups. Sensors based on there nanorods with smaller diameters had a better sensitivity due to increasing oxygen vacancies and larger effective surface area. Therefore, developing simple methods that can synthesize large amounts of nanostructured ZnO materials with desired sizes to utilize for high-sensitivity and low-cost gas sensors have still remained a significant challenge.

In this paper, we reported NO_2 sensors based on the ZnO nanorods with different sizes fabricated using a simple hydrothermal method without surfactants. The sensors offered the excellent response and sensitivity to NO_2 at very low concentrations as low as 100 ppb. The influence of the size of the ZnO nanorods on the NO_2 sensing response was focused.

2. Experiment

2.1. Synthesis of ZnO nanorods

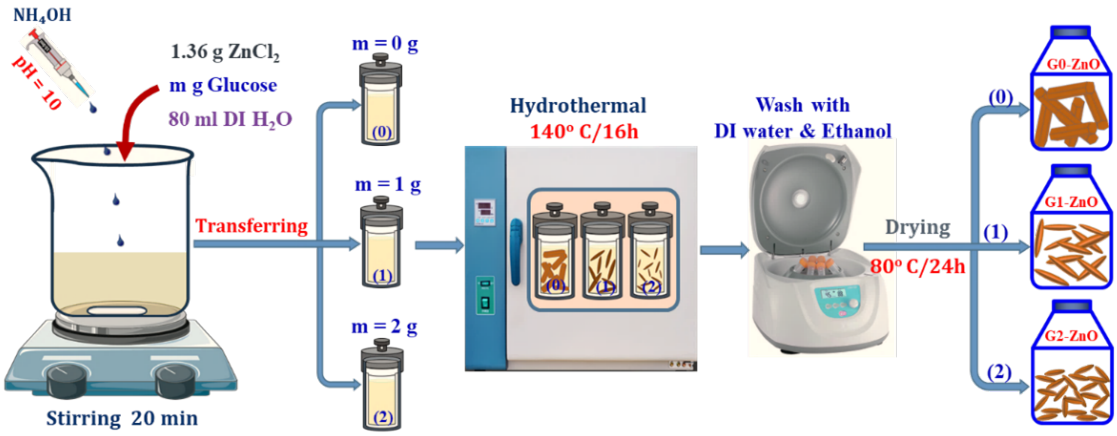

Scheme 1. Process of synthesizing the ZnO nanorods with different sizes by hydrothermal method.

All precursors were analytical grade and purchased without further purification, including zinc chloride, D-Glucose, ammonium solution, and ethanol from Sigma–Aldrich Company, Ltd. (USA). Nanorods ZnO with different sizes were fabricated by a simple hydrothermal method. Scheme 1 introduces the hydrothermal process to fabricate the ZnO nanorods of different sizes. Briefly, a magnetic stirrer dissolved $ZnCl_2$ (1.36g) and amounts of D-Glucose (0.0 g, 1.0 g, and 2.0 g) in 80 ml of deionization of water. Herein, the different D-Glucose concentrations were used to control size of the obtained ZnO nanorods. Next, adding ammonium solution drop by drop into the mixtures to maintain pH of about 10. Then, each solution mixture was put into a 100ml Teflon-lined stainless-steel autoclave and sealed. The sealed autoclaves were placed in an electric oven

and set at 140 ˚C for 16 h for hydrothermal process. After the hydrothermal time, the electric oven automatically was shut off and naturally cooled to room temperature. The products in the three reaction flasks were washed with deionized water and ethanol by using a centrifuge to separate particles. Finally, the products were air-dried at 80˚C for 24 h before fabricating sensor devices.

2.2. Sensor fabrication and gas-sensitive characteristics

The gas sensors in this study were fabricated by using the thick film technique [19]. Specifically, 5 mg of each sample of the synthesized ZnO nanorods of each was dispersed in ethanol solution by low-intensity ultrasonic vibration. Then, the mixture was dropped on a pair of comb-type Pt interdigital electrode and dried before heat treatment at 550˚C for 2 h in air. The fabricated sensors are denoted as G0-ZnO, G1-ZnO, and G2-ZnO for the used D-Glucose concentrations (0.0 g, 1.0 g, and 2.0 g) in the hydrothermal synthesis, respectively. To measure the gas-sensing properties, the sensor were placed atop heating plate with a temperature controller. The sensors's resistance was continuously recorded with Keithley instrument (Model - 2602) when responding to dry air and tested gases. Herein, using a gas mixing system, NO_2 concentrations in the tested gases can be generated by varying the mixing ratio of the standard gas (100 ppm NO_2) with dry air [20]. The sensing response of the sensors is defined as $S = R_{gas}/R_{air}$ for oxidizing gases and $S = R_{air}/R_{gas}$ for reducing gases (where R_{air} is the sensors's resistance in dry air, and R_{gas} is the sensors's resistance in tested gas).

2.3. Material characterization

The crystal structure of the synthesized samples was investigated by the X-ray diffraction (XRD, Bruker D8 Advance), operating at 40 kV and 40 mA using Cu-K radiation ($\lambda = 1.54178$ Å) in the 2θ range of 20˚– 80˚. The morphologies of the synthesized samples were studied by the field emission scanning electron microscope (FE-SEM; JEOL model 7600F). The atomic compositions of the synthesized samples were analyzed by the energy-dispersive X-ray (EDX) spectroscopy.

3. Results and discussion

3.1. Morphology and structure

The morphologies of the material samples after heat treatment at 550 ˚C were studied by FE-SEM images. Figures 1(A-B) indicated low and high-magnification FE-SEM images of the synthesized sample without D-Glucose (G0-ZnO). The result in Fig. 2A showed that the morphology is uniform rods with a regular hexagonal cross-section. The average length and diameter of these rods estimated from the FE-SEM images are about 8 *mu*m and 1.6 *mu*m, respectively. The high-magnification FE-SEM image (Fig. 1B) showed that the nanorod tips are relatively flat, and its surrounding surface was not smooth.

In the synthetic samples with using D-Glucose, the collected nanorods were much smaller than those in the synthetic sample without using D-Glucose. Figures 1(D-E) are low and high-magnification of the FE-SEM images of the fabricated sample with using 1g of D-Glucose. The results showed that the obtained morphology of this sample is relatively uniform nanorods (Fig. 1D). These nanorods are not linked and their observed length and diameter are about 800 nm and 120 nm, respectively, and the nanorods tend to be tapered (Fig. 1E). The FE-SEM images of the fabricated nanorods with 2 g of D-Glucose were shown in Figs. 1(G-H). These nanorods are smaller

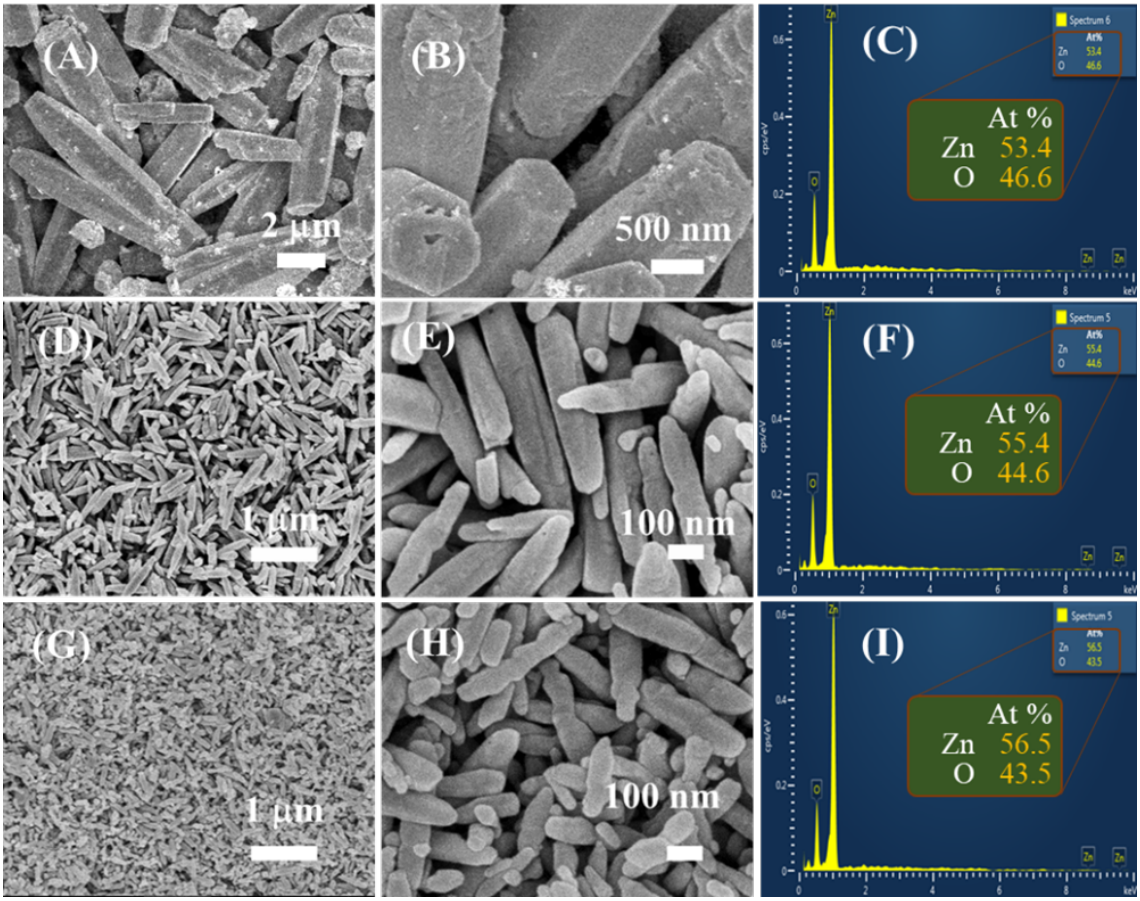

Fig. 1. FE-SEM images and EDX spectra of the ZnO nanorods fabricated with using different amounts of Glucose after heating at 550 ˚C for 2h in air: (A, B, C) G0-ZnO; (D, E, F) G1-ZnO; (G, H, I) G2-ZnO.

in length and diameter than those of the fabricated nanorods with using 1 g of D-Glucose. The average length and diameter calculated from the FE-SEM images for the sample G2-ZnO are about 400 nm and 90 nm, respectively (Fig. 1H). This result indicated that the sizes of these nanorods are significantly reduced in comparison with those of the fabricated nanorods without D-Glucose (with length ~8 mm and diameter ~1.6 mm). Therefore, the used amounts of D-Glucose played an important role in controlling the sizes of the ZnO nanorods. As the D-Glucose concentration increased, the fabricated ZnO nanorods reduced their sizes. As the size of the nanorods decreases, the specific surface area increases, increasing number of adsorption gas molecules on the nanorods surface, which can improve the gas sensing response.

The elemental compositions of the nanorods fabricated with different amounts of D-Glucose were conducted through EDX measurement. Figures 1(C, F, I) are the EDX spectrum of the samples of G0-ZnO, G1-ZnO, and G2-ZnO, respectively. The EDX spectroscopy results showed that the samples consisted of only Zn and O elements, and no other impurity elements were observed.

Therefore, the fabricated ZnO nanorods presented a purity. The elemental ratios of of [O]/[Zn] of the nanorods samples of G0-ZnO, G1-ZnO, and G2-ZnO are 46.6/53.4, 44.6/55.4 and 43.5/56.4, respectively. These ratios are all less than that of the stoichiometric formula of ZnO ([O]/[Zn] = 1.0). It is provided that the fabricated nanorods can be more oxygen vacancies, therefore, the ZnO nanorods are expected as *n*-type semiconductor when applied to the gas sensors.

The X-ray diffraction patterns of the samples G0-ZnO, G1-ZnO, and G2-ZnO after heat treatment at 550˚C for 2h were shown in Fig. 2. All the sample's diffraction peaks coincided with the standard card JCPDS Card No. 16-0161 profile of the hexagonal (wurtzite) crystal structure of ZnO. In addition, no other impurity diffraction peak was observed from the XRD patterns, indicating that the fabricated ZnO nanorods had a single-phase hexagonal crystal structure. The strong and sharp diffraction peaks also show the ZnO nanorods having high crystallinity. Using the Scherrer equation $D = 0.89\lambda/\beta\cos(\theta)$ where λ is the Cu-Kα X-radiation with a wavelength of approximately 1.542 Å, β is the full width at half maximum of the diffraction peaks in radians, and θ is the Bragg angle), we calculated the average crystal size of the ZnO nanorods of G0-ZnO, G1-ZnO, and G2-ZnO to be about 31.54 nm; 24.36 nm and 21.75 nm, respectively. These values are smaller than the diameters of the nanorods, indicating that the ZnO nanorods obtained after heat treatment are polycrystalline.

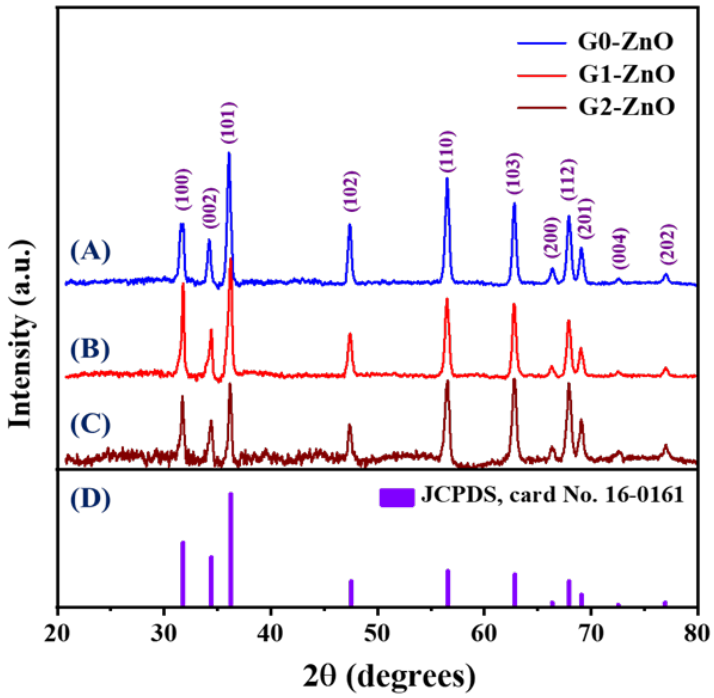

Fig. 2. XRD patterns of the ZnO nanorods after heating at 550 ˚C for 2h in the air: (A) G0-ZnO; (B) G1-ZnO; (C) G2-ZnO and (D) Purple lines showed as the standard pattern profile of hexagonal structure of ZnO.

3.2. Gas sensing properties

The NO_2 gas-sensing characteristics of the fabricated sensors of G0-ZnO, G1-ZnO, and G2-ZnO were investigated for responding to the gas concentrations at different operating temperatures. Figures 3 (A-C) show the NO_2 gas-sensing properties of the G2-ZnO sensor based on ZnO nanorods fabricated with 2 g of D-Glucose. Fig. 3A showed the resistance changes of the G2-ZnO sensor versus different NO_2 concentrations at working temperatures of 100˚C, 150˚C, 200˚C, and 250˚C. At all the operating temperatures, the G2-ZnO sensor can detect very low NO_2 concentrations (as low as 100 ppb). The sensor's resistance significantly increases when exposed to NO_2 gas and recovers to its original value upon re-exposure to dry air for all the tested concentrations. This result provided that the process of adsorption and desorption of NO_2 gas on the surface of ZnO nanorods is considered to be a reversible process. This behavior is similar to the report [21] on the NO_2 gas-sensitive properties of ZnO nanorods as properties of n-type semiconductors.

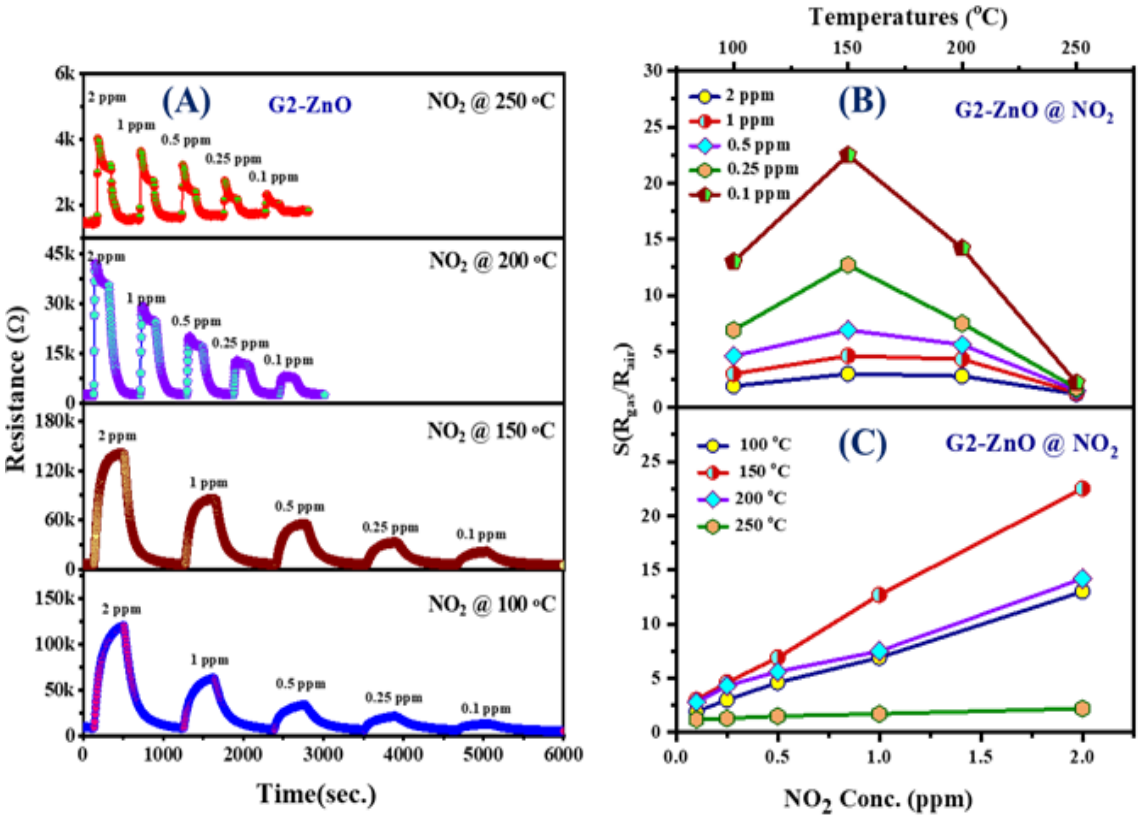

Fig. 3. The NO_2 sensing responses of the G2-ZnO sensor: (A) the change in resistance upon exposure to different concentrations of NO_2 at 100, 150, 200, and 250˚C; (B) temperature dependence, and (C) concentration dependence.

Figure 3B shows the response of the G2-ZnO sensor to the temperature measured at concentrations of 0.1, 0.25, 0.5, 1.0, and 2 ppm NO_2. The sensor exhibits the highest response at

150˚C working temperature for all investigated NO_2 concentrations. The optimal working temperature of the G2-ZnO sensor in this study is about 50˚C lower than that of the sensor using ZnO nanorods synthesized by hydrothermal growth [9]. Fig. 3C also shows that the sensor response is relatively linear to NO_2 in the concentration range from 0.1 to 2 ppm. The sensor's sensitivity can be calculated from the slopes of the response lines of approximately 6.9 ppm^{-1}, 12.7 ppm^{-1}, 7.5 ppm^{-1}, and 1.7 ppm^{-1} at operating temperatures of 100˚C, 150˚C, 200˚C, and 250˚C, respectively.

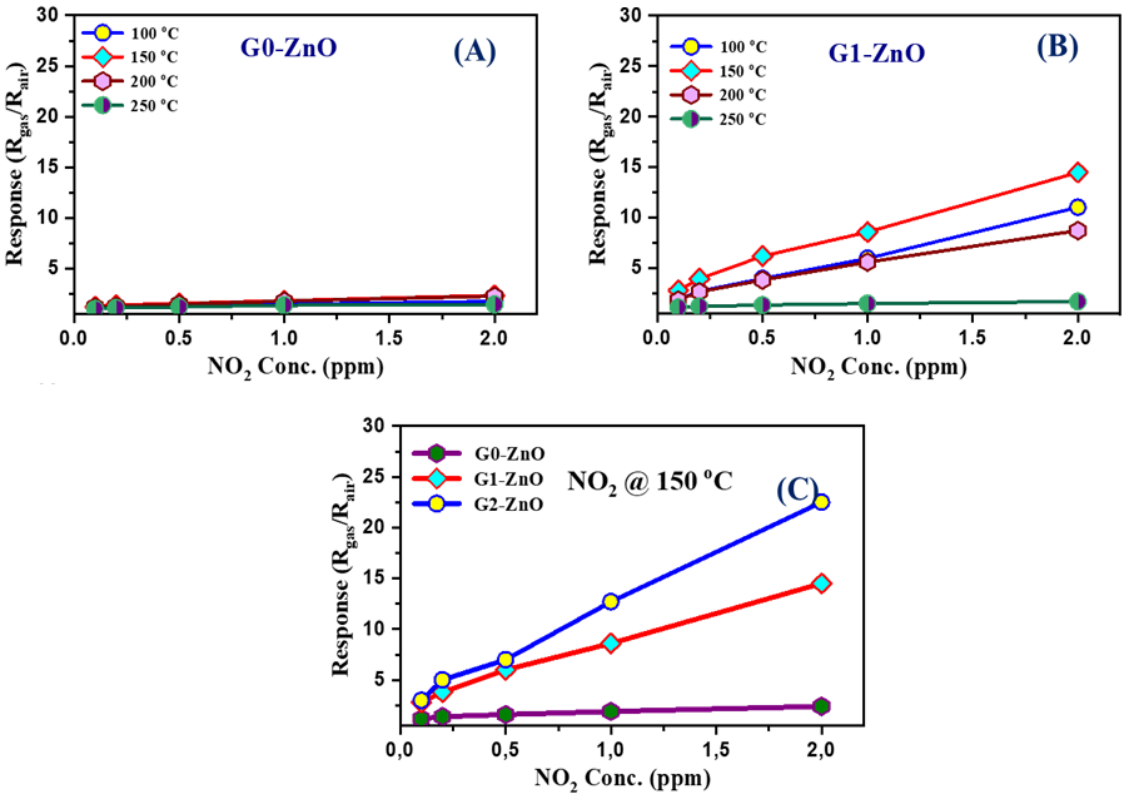

Fig. 4. The sensing responses as a function of NO_2 concentration measured at different temperatures: (A) sensor G0-ZnO, (B) sensor G1-ZnO anh (C) Comparison of the response of G0-ZnO, G1-ZnO, and G2-ZnO at 150˚C.

The NO_2 gas-sensing characteristics of the G0-ZnO and G1-ZnO sensors exhibit the same trend as the G2-ZnO sensor. Figures 4A and B show the response of G0-ZnO and G1-ZnO sensors to NO_2 concentration at operating temperature values of 100˚C, 150˚C, 200˚C, and 250˚C. Both sensors can detect NO_2 in a 0.1 to 2 ppm concentration range. However, the G1-ZnO sensor based on the smaller ZnO nanorods has a much higher response than the G0-ZnO sensor. Compare the response of the sensors G0-ZnO, G1-ZnO, and G2-ZnO to the NO_2 gas concentration at the optimal operating temperature of 150˚C (Fig. 4C). The G2-ZnO sensor exhibits the highest response and sensitivity. The result can be explained by the ZnO nanorods with the smallest size, creating number of the gas adsorption sites on the surface of the ZnO nanorods, thus improving the sensing response.

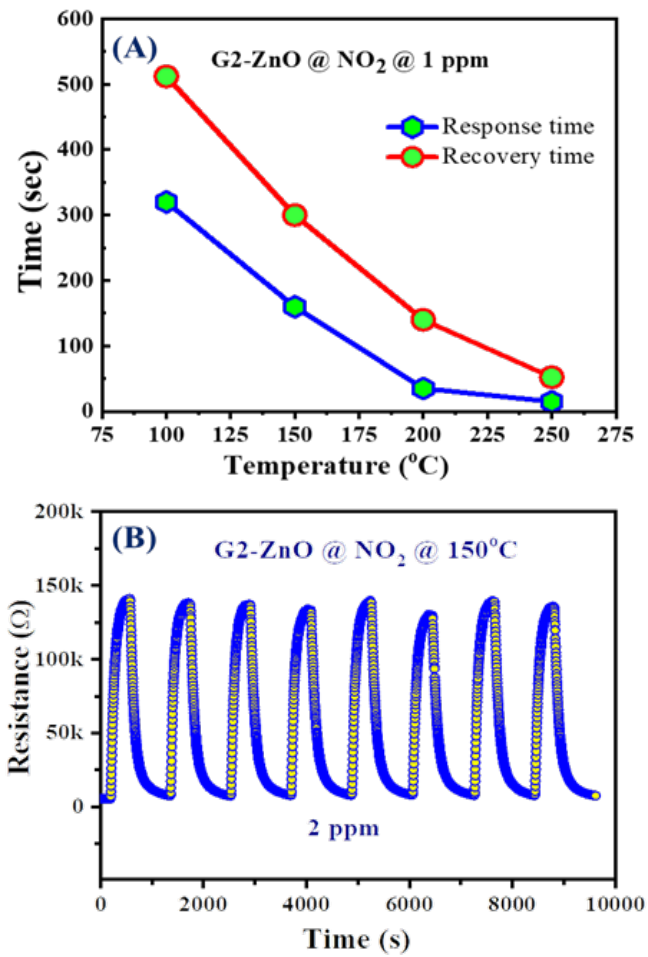

Fig. 5. NO_2 sensing characteristics of the G2-ZnO sensor: (A) response and recovery times as a function of working temperatures measured at 1 ppm concentration; (B) repeatability of the sensor at 2 ppm concentration at optimum working temperature.

Figure 5A shows the response and recovery times of the G2-ZnO sensor calculated from the resistance data to time at 1 ppm NO2 concentrations at the operating temperatures of 100˚C, 150˚C, 200˚C and 250˚C. The recovery response time decreased rapidly as the operating temperature increased. At the optimum operating temperature of 150˚C, the response and recovery times of the sensor are 160 s and 302 s, respectively. This result showed that this sensor can be used to online monitor NO_2 pollution in the environment. Fig. 6B showed the repeatability of the G2-ZnO sensor responded to 2 ppm NO_2 concentration at the optimum operating temperature of 150˚C. The results showed that the sensor exhibits an excellent repeatability after eight on/off cycles of dry air and NO_2. Therefore, it provides that the adsorption and desorption of NO_2 gas molecules on the surface of ZnO nanorods are more reversible.

Table 1 showed the NO_2 sensing response when compared with ZnO nanostructures between our typical research result and other reports. It was obvious that the ZnO nanorods in this work exhibited the highest sensing response in compared with the other morphologies of the nanowire arrays, nanosheets, nanoneedles, nanowire arrays, and thin film.

Table 1. Summary of the NO_2 sensing response of the ZnO nanostructures with different morphologies.

Materials	Operating temp.	Conc. (ppm)	Response ($S = R_{air}/R_{gas}$)	Refs.
ZnO Nanoparticles	250˚ C	0.5	14	[22]
ZnO nanowire arrays	250˚ C	5	3.5	[23]
ZnO nanosheets	170˚C	50	10.2	[24]
ZnO nanoneedles	200˚C	8.5	1.8	[25]
ZnO thin film	200˚C	100	1.4	[26]
ZnO nanorods	**150**˚C	0.1 0.5 1 2	3.1 6.9 12.7 22.5	**This work**

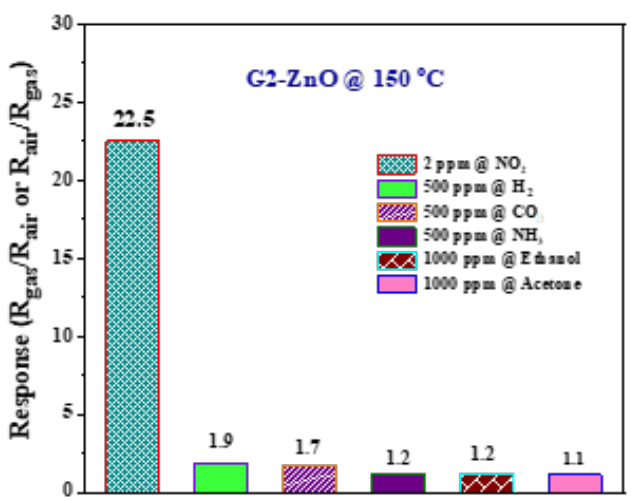

Fig. 6. Selectivity of the G2-ZnO sensor to different gases measured at 150˚ C.

The selectivity is an essential parameter of gas sensors for practical applications. Fig. 6 showed the selectivity of the G2-ZnO sensor for detecting some gases (including NO_2, H_2, CO, NH_3, Ethanol, and Acetone), that was investigated at the optimum operating temperature for NO_2 gas. The results showed that the sensor exhibited a superior sensing response to NO_2 gas in compared to the other gases. Indeed, the response for 2 ppm NO_2 concentration was 22.5 while those for 500 ppm H_2, 500 ppm CO, 500 ppm NH_3, 1000 ppm Ethanol, and 1000 ppm Acetone

were only 1.9, 1.7, 1.2, 1.2, and 1.1, respectively. It indicated that the G2-ZnO sensor based on the ZnO nanorods fabricated form the hydrothermal method using 2g D-Glucose has an excellent NO_2 selectivity compared to the other investigated gases.

3.3. Gas sensing mechanism

A schematic diagram illustrates that was proposed for the gas sensing mechanism due to changing in depletion layer width of the ZnO nanorods when exposed to NO_2 oxidizing gas as depicted in Fig. 7. This mechanism describes the adsorption and desorption of gases on the surface of the ZnO nanorods. Before exposure to NO_2, oxygen molecules in the air adsorbed on the surface and captured electrons in the conduction band, forming a depletion layer on the surface of the ZnO nanorods (Fig. 7A). The oxygen adsorbed on the surface of ZnO nanorods can be described by the following reaction equations [15]:

$$O_2\,(\text{gas}) \rightarrow O_2(ads) \tag{1}$$

$$O_2\,(\text{ads}) + e^- \rightarrow O_2^-\,(\text{ads}) \tag{2}$$

When the sensor is exposed to NO_2 gas, the gas molecules can directly adsorb on the surface of the ZnO nanorods or react with the adsorbed oxygen ions, as described by the following equations [15, 27].

$$NO_2(\text{gas}) + e^- \rightarrow NO_2^-(\text{ads}) \tag{3}$$

$$NO_2^-\,(\text{ads}) + O_2^-\,(\text{ads}) + e^- \rightarrow 2O^-\,(\text{ads}) + NO_2^-(\text{ads}) \tag{4}$$

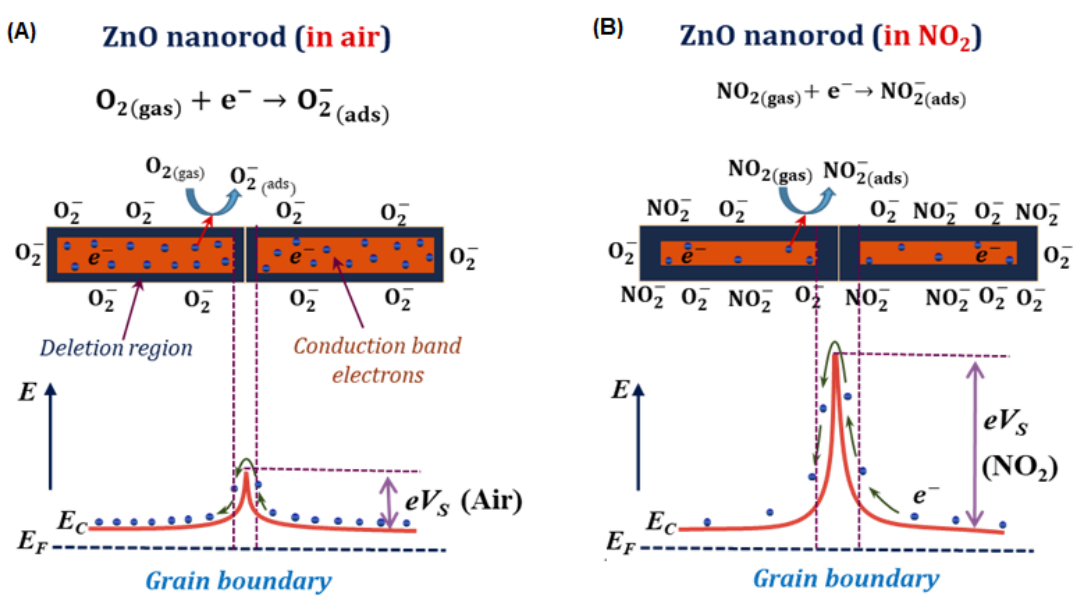

Fig. 7. Illustration of NO_2 gas sensing mechanism of the ZnO nanorods based sensor.

Therefore, when the NO_2 gas molecules are adsorbed on the surface of the nanorods, numerous electrons in the conduction band are captured, and the thickness of the depletion region increases,

increasing the barrier height (Fig. 7B), resulting in the resistance of the sensor increases. In addition, because the ZnO nanorods have oxygen vacancies (*n*-type semiconductors) and surface defects, which are the favoured adsorption sites of oxygen and NO_2 gas molecules, the sensor response is improved. Small-sized nanorods will have a large specific surface area, leading to many gas adsorption centers, increasing the number of surface-adsorbed gas molecules can improve the sensor response.

4. Conclusion

This paper introduces the fabrication process of ZnO nanorods with different sizes controlled by a simple hydrothermal method without using any surfactants for NO_2 gas sensing applications. The length and diameter of the ZnO nanorods can be easily controlled by varying the D-Glucose concentration in the hydrothermal process. The ZnO nanorods (length ~400 nm and diameter ~ 90 nm) synthesized with the content of 2 g D-Glucose have an excellent performance for fabricating low-cost NO_2 gas sensors. These ZnO nanorods can detect toxic gases NO_2 at low concentrations below 100 ppb. In addition, the sensor based on ZnO nanorods exhibits the high response, sensitivity, repeatability, and selectivity to NO_2. The sensor response to 2 ppm NO_2 was higher than 11.8, 13.3, and 18.8 with 500 ppm of H_2, CO, and NH_3 gases, respectively. Our research results show that the sensor based on ZnO nanorods can be applied to detect NO_2 toxic gas in the air, in industry, medical, and military.

Acknowledgment

This research is funded by Ministry of Education and Training under grand number B2022-XDA-11.

References

[1] Ü. Özgür, Y. I. Alivov, C. Liu, A. Teke, M. A. Reshchikov, S. Doğan *et al.*, *A comprehensive review of zno materials and devices*, J. Appl. Phys. **98** (2005) 041301.

[2] Y. Kang, F. Yu, L. Zhang, W. Wang, L. Chen and Y. Li, *Review of ZnO-based nanomaterials in gas sensors*, Solid State Ion. **360** (2021) 115544.

[3] Z. Liu, L. Yu, F. Guo, S. Liu, L. Qi, M. Shan *et al.*, *Facial development of high performance room temperature NO_2 gas sensors based on ZnO nanowalls decorated rgo nanosheets*, Appl. Surf. Sci. **423** (2017) 721.

[4] D. Zhang, Y.-H. Liu and L. Zhu, *Surface engineering of ZnO nanoparticles with diethylenetriamine for efficient red quantum-dot light-emitting diodes*, iScience **25** (2022) 105111.

[5] R. Dash, C. Mahender, P. Kumar Sahoo and A. Soam, *Preparation of zno layer for solar cell application*, Materials Today: Proceedings **41** (2021) 161.

[6] B. Yuliarto, M. F. Ramadhani, Nugraha, N. L. W. Septiani and K. A. Hamam, *Enhancement of so 2 gas sensing performance using zno nanorod thin films: The role of deposition time*, Journal of Materials Science **52** (2017) 4543.

[7] V. Dhingra, S. Kumar, R. Kumar, A. Garg and A. Chowdhuri, *Room temperature SO_2 and H_2 gas sensing using hydrothermally grown GO–ZnO nanorod composite films*, Mater. Res. Express **7** (2020) 065012.

[8] L. H. Minh, P. T. Thuy Thu, B. Q. Thanh, N. T. Hanh, D. T. Thu Hanh, N. Van Toan *et al.*, *Hollow zno nanorices prepared by a simple hydrothermal method for no2 and so2 gas sensors*, RSC Adv. **11** (2021) 33613.

[9] F.-T. Liu, S.-F. Gao, S.-K. Pei, S.-C. Tseng and C.-H. J. Liu, *Zno nanorod gas sensor for no2 detection*, J. Taiwan Inst. Chem. Eng. **40** (2009) 528.

[10] P. S. Venkatesh, P. Dharmaraj, V. Purushothaman, V. Ramakrishnan and K. Jeganathan, *Point defects assisted nh3 gas sensing properties in zno nanostructures*, Sens. Actuators B Chem. **212** (2015) 10.

[11] N. D. Khoang, H. S. Hong, N. Van Duy, N. D. Hoa, D. D. Thinh, N. Van Hieu *et al.*, *On-chip growth of wafer-scale planar-type ZnO nanorod sensors for effective detection of CO gas*, Sens. Actuators B Chem. **181** (2013) 529.

[12] G. Agarwal and R. Speyer, *Current change method of reducing gas sensing using zno varistors*, J. Electrochem. Soc. **145** (1998) 2920.

[13] R. Gao, X. Cheng, S. Gao, X. Zhang, Y. Xu, H. Zhao *et al.*, *Highly selective detection of saturated vapors of abused drugs by zno nanorod bundles gas sensor*, Appl. Surf. Sci. **485** (2019) 266.

[14] W. Liu, Z. Chen, X. Si, H. Tong, J. Guo, Z. Zhang *et al.*, *Facile synthesis of pt catalysts functionalized porous zno nanowires with enhanced gas-sensing properties*, J. Alloys Compd. **947** (2023) 169486.

[15] M. Sik Choi, M. Young Kim, A. Mirzaei, H.-S. Kim, S. il Kim, S.-H. Baek *et al.*, *Selective, sensitive, and stable no2 gas sensor based on porous zno nanosheets*, Appl. Surf. Sci. **568** (2021) 150910.

[16] Z. Fan and J. G. Lu, *Chemical sensing with ZnO nanowire*, 5th IEEE Conference on Nanotechnology **1** (2005) 403.

[17] M. Jiao, N. Van Duy, D. D. Trung, N. D. Hoa, N. Van Hieu, K. Hjort *et al.*, *Comparison of no 2 gas-sensing properties of three different zno nanostructures synthesized by on-chip low-temperature hydrothermal growth*, J. Electron. Mater. **47** (2018) 785.

[18] L. Liao, H. B. Lu, J. C. Li, H. He, D. F. Wang, D. J. Fu *et al.*, *Size dependence of gas sensitivity of ZnO nanorods*, J. Phys. Chem. C **111** (2007) 1900.

[19] P. Van Tong, L. Hoang Minh, N. Van Duy and C. Manh Hung, *Porous In_2O_3 nanorods fabricated by hydrothermal method for an effective CO gas sensor*, Mater. Res. Bull. **137** (2021) 111179.

[20] P. Van Tong, N. D. Hoa, N. Van Duy, D. T. T. Le and N. Van Hieu, *Enhancement of gas-sensing characteristics of hydrothermally synthesized WO_3 nanorods by surface decoration with pd nanoparticles*, Sens. Actuators B Chem. **223** (2016) 453.

[21] J. Xuan, G. Zhao, M. Sun, F. Jia, X. Wang, T. Zhou *et al.*, *Low-temperature operating zno-based no2 sensors: a review*, RSC Adv. **10** (2020) 39786.

[22] C. T. Quy, N. X. Thai, N. D. Hoa, D. T. Thanh Le, C. M. Hung, N. Van Duy *et al.*, *C2h5oh and no2 sensing properties of zno nanostructures: correlation between crystal size, defect level and sensing performance*, RSC Adv. **8** (2018) 5629.

[23] X. Chen, Y. Shen, W. Zhang, J. Zhang, D. Wei, R. Lu *et al.*, *In-situ growth of zno nanowire arrays on the sensing electrode via a facile hydrothermal route for high-performance no2 sensor*, Appl. Surf. Sci. **435** (2018) 1096.

[24] T. A. Kusumam, V. Siril, K. Madhusoodanan, M. Prashantkumar, Y. Ravikiran and N. Renuka, *NO_2 gas sensing performance of zinc oxide nanostructures synthesized by surfactant assisted low temperature hydrothermal technique*, Sens. Actuators A Phys. **318** (2021) 112389.

[25] R. C. Pawar, J.-W. Lee, V. B. Patil and C. S. Lee, *Synthesis of multi-dimensional zno nanostructures in aqueous medium for the application of gas sensor*, Sens. Actuators B Chem. **187** (2013) 323.

[26] A. Z. Sadek, S. Choopun, W. Wlodarski, S. J. Ippolito and K. Kalantar-zadeh, *Characterization of zno nanobelt-based gas sensor for* h_2, no_2, *and hydrocarbon sensing*, IEEE Sens. J. **7** (2007) 919.

[27] R. R. Kumar, T. Murugesan, A. Dash, C.-H. Hsu, S. Gupta, A. Manikandan *et al.*, *Ultrasensitive and light-activated no2 gas sensor based on networked mos2/zno nanohybrid with adsorption/desorption kinetics study*, Appl. Surf. Sci. **536** (2021) 147933.